AD-A171 847 EMISSION BEHAVIOR OF FLAWED UNIDIRECTIONAL CARBON FIBER - EPOXY COMPOSITES(U) CALIFORNIA UNIV LOS ANGELES DEPT OF MATERIALS SCIENCE AND ENG.. K ONO JUL 86 TR-86-01 1/1

UNCLASSIFIED N00014-81-K-0011 F/G 11/4 NL

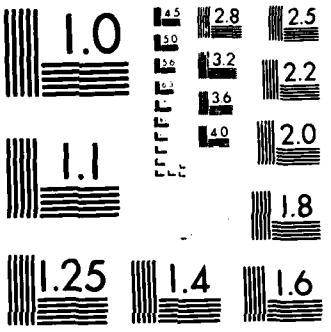

SECURITY CLASSIFICATION OF THIS PAGE (When Data Entered)

REPORT DOCUMENTATION PAGE

READ INSTRUCTIONS BEFORE COMPLETING FORM

1. REPORT NUMBER: 86-01	2. GOVT ACCESSION NO.
3. RECIPIENT'S CATALOG NUMBER	
4. TITLE (and Subtitle): Emission Behavior of Flawed Unidirectional Carbon Fiber - Epoxy Composites	5. TYPE OF REPORT & PERIOD COVERED: Technical
6. PERFORMING ORG. REPORT NUMBER	
7. AUTHOR(s): Kanji Ono	8. CONTRACT OR GRANT NUMBER(s): N00014-81-K-0011
9. PERFORMING ORGANIZATION NAME AND ADDRESS: University of California, Los Angeles, California, 90024	10. PROGRAM ELEMENT, PROJECT, TASK AREA & WORK UNIT NUMBERS
11. CONTROLLING OFFICE NAME AND ADDRESS: Physics Division Code 412, Office of Naval Research, Arlington, Virginia 22217	12. REPORT DATE: July 1986
	13. NUMBER OF PAGES: 7
14. MONITORING AGENCY NAME & ADDRESS (if different from Controlling Office): Office of Naval Research Branch Office, 1030 East Green Street, Pasadena, California 91101	15. SECURITY CLASS. (of this report): Unclassified
	15a. DECLASSIFICATION DOWNGRADING SCHEDULE

16. DISTRIBUTION STATEMENT (of this Report)

Approved for Public release, distribution unlimited

17. DISTRIBUTION STATEMENT (of the abstract entered in Block 20, if different from Report)

18. SUPPLEMENTARY NOTES

Published in Proc. Second International Symposium on Acoustic Emission from Reinforced Composites

19. KEY WORDS (Continue on reverse side if necessary and identify by block number)

Acoustic Emission
Delamination
Fiber Fracture
Amplitude Distribution
Carbon Fiber-Epoxy Composites

20. ABSTRACT (Continue on reverse side if necessary and identify by block number)

See Next Page

DD FORM 1 JAN 73 1473 EDITION OF 1 NOV 65 IS OBSOLETE

SECURITY CLASSIFICATION OF THIS PAGE (When Data Entered)

SECOND INTERNATIONAL

Symposium on Acoustic Emission From Reinforced Composites

MONTREAL, CANADA

JULY 21-25, 1986

The Society of the Plastics Industry, Inc.
Reinforced Plastics/Composites Institute

KANJI ONO*

Acoustic Emission Behavior of Flawed Unidirectional Carbon Fiber-Epoxy Composites

ABSTRACT

This paper reports an experimental investigation on mechanical and acoustic emission behavior of specially designed and manufactured carbon fiber epoxy composites. Unidirectional composite laminates with various flaw configurations were tested in tension and their mechanical and acoustic emission responses were determined. Fiber fracture, delamination, splitting (or cracking along fibers) and friction of delaminated faces contributed to characteristic acoustic emission behavior. These can be discriminated on the basis of peak amplitude and event duration of observed acoustic emission signals.

The short duration ($< 100\ \mu s$), lower amplitude signals (< 50 dB) signify carbon fiber fracture, while the medium amplitude signals (50 – 70 dB) with an average event duration of ~120 μs indicate the initiation and slow growth of delamination. High amplitude events (> 70 dB) have long (> 200 μs) event durations and are caused by rapid advances of delamination. Splitting or cracking along the fibers produces low to medium amplitude events with a long event duration (> 100 μs). This type of acoustic emission signals has overlapping characteristics with those of delamination and needs further delineation of distinguishing parameters. Delaminated samples also emit acoustic emission signals with amplitudes in the range of 40 – 50 dB and event duration of < 150 μs. These appear to arise from the friction of delaminated faces.

This research was supported by Hughes Aircraft Co. and by the Office of Naval Research.

INTRODUCTION

Acoustic emission studies of composite materials have been numerous. Over 200 papers have been published by 1983 [1] and a comparable number of papers have since been published. In the case of fiber reinforced composites, however, a basic understanding is still limited. For example, it is not certain whether the fracture of a fiber produces high amplitude acoustic emission or not. In order to utilize computerized pattern recognition analysis procedures for quality assurance and for nondestructive testing [2–4], it is necessary to characterize acoustic emission parameters for a given fracture mechanism.

An even larger number of papers have been published on failure modes of composites. In particular, the fracture of flawed composites and the delamination of laminated composites have attracted recent attention [5–7]. Some studies, e.g. Reference [8], have focused on the acoustic emission due to damage growth. However, the typically complex lay-up sequences and the lack of pre-existing flaws in most studies have complicated the interpretation of acoustic emission observation. While the clarification of fracture processes in complex composite lay-ups using acoustic emission is the final goal, initially we need simple material systems to understand acoustic emission behavior of various composite materials. For this purpose, unidirectional composites are needed with some laminae cut at specific locations. This type of composite must be produced in-house since no such material is commercially available. For unidirectional composites, fiber fracture and matrix fractures, i.e., delamination and splitting, are expected. All three types are observed in the present study. In order to evaluate acoustic emission parameters associated with specific failure mechanisms, advanced acoustic emission instrumentation is used to determine signal amplitude, rise time, signal duration, event rates and their distributions. Results are correlated to fracture behavior of these model composites.

EXPERIMENTAL DESIGN

Two basic types of samples were employed. One is to embed pre-cut laminae within unidirectional tensile samples. Pre-cut laminae were placed on the outer surfaces (symmetrically) or in the center. This group of sample geometries is expected to generate stress concentration at the pre-cut laminae, leading to fiber fracture. The pre-existing flaws are also expected to initiate delamination. During testing, the outer pre-cut laminae delaminated, making a comparison of acoustic emission test results difficult. Thus, pre-cut laminae were in most cases placed inside. The other type of samples has all the laminae pre-cut with 1/2 to 2″ overlap. These are similar to lap joints. Most of the samples in this group had the overlap length of 1″. These pre-cut laminae were grouped into two or three groups, each one to six laminae thick. In this type of sample geometries, delamination is expected to be the primary failure mode.

EXPERIMENTAL PROCEDURES

Materials

Carbon fiber reinforced epoxy matrix composite sheets were produced by thermal compression method from a prepreg. Rolls of 6″ wide prepreg were obtained from Hexcel and kept in a freezer. Reinforcing fibers were Celion G-50 and the matrix was Hexcel F584 epoxy. Specifications are given in Table 1. Required numbers of unidirectional laminae were cut to 10″ long and stacked according to design. Typically, 6″ × 10″ size sheets were produced. The stacked laminae were sandwiched between release sheets and bleeder clothes and placed in a hot platen press. Under a pressure

*Department of Materials Science and Engineering, School of Engineering and Applied Science, University of California, Los Angeles, California 90024, U.S.A.

of 100 psi, press temperature was increased to 350°F at a heating rate of 5°F/min. Hold time at 350°F was 2 hours.

Tensile samples were prepared from these unidirectional composite sheets. Nominal width of 1/2" was used. Only the fiber direction (0°) samples were made and their length was 10". Reinforcing tabs, 3" long, were glued to each end using cyanoacrylic glue. The reinforcing tabs were tapered on one end and made of 1/4" thick PVC. The thickness of a sample was dependent on the number of laminae with a single lamina thickness of typically 0.005".

Including materials prepared for preliminary testing, a total of 35 composite sheets were prepared. Of these, the main part of this study employed fourteen sheets, eight of which had some uncut laminae. The remaining six had all the laminae pre-cut. The length of overlap ranged from 1/2" to 2" and was 1" in four of the six sheets. Ply configurations are given in Table 2.

Testing

The mechanical testing was performed using a floor model Instron. Screw-assisted wedge grips were used to hold a sample. A crosshead speed of 0.01"/min was always used. Since the tested section has 4" length, the nominal strain rate was 4.1×10^{-5}/s. However, this value is unreliable because of the presence of flaw(s) in a sample. Tests were conducted in room air at 70 to 75°F. Humidity was not controlled.

Acoustic emission tests were conducted during tensile testing. An acoustic emission sensor (AET MAC175L) was placed on a sample at the center portion using a viscous couplant and springs. Two sensors were used in the course of acoustic emission tests. One of them had a peak sensitivity of 70 dB in reference to 1V per μbar and was more sensitive than the other by 33 dB. The less sensitive sensor was useful to evaluate high amplitude acoustic emission signals. The sensor output was fed to a preamplifier We used one or two preamplifiers with a plug-in filter of 125 to 250 kHz. These were 60 dB or 40 dB gain preamplifiers (AET 160B or 140A). The high gain preamplifier was used when low amplitude signals needed to be resolved. Since the dynamic range of signal processing circuit is limited to about 60 dB, the use of the 60 dB preamplifier precludes the characterization of signals above 78 dB in reference to 1 μV (i.e., the signal level of 8 mV or higher at the sensor output). The use of the low sensitivity sensor and 40 dB gain preamplifier allowed the detection of signals up to 131 dB.

The preamplifier output was fed to a microprocessor-based acoustic emission signal processor (AET Model 5000A). Although two inputs can be processed, only one input was processed in most tests, in order to gain a higher processing speed. This signal processor records the peak amplitude, signal duration, signal rise time, ringdown or acoustic emission counts of each burst-type acoustic emission signal. The rate of burst-emission signals and applied load can be recorded as a function of time. After a test, distributions (cumulative or differential) of these acoustic emission parameters can be obtained from a specific portion of the test. In addition, cross-plots of several parameters can be made; e.g., the peak amplitude vs. signal duration. In this case, a dot is imprinted for each burst-emission signal. The processed data is stored on a hard disk during a test and later stored on a floppy disk. The rms voltages of acoustic emission signals were also recorded using two rms voltmeters, a multi-channel digital storage recorder and a two-pen recorder.

RESULTS AND DISCUSSION

Fracture Modes and Strength

Three main modes of fracture were observed. The first type is fiber fracture at a pre-cut lamina location. (When individual fibers fail at random locations, no observable indication is produced on the sample surface or on the load-time curve. We will discuss this type of fiber fracture later.) The second is splitting parallel to the load (or fiber) direction, followed by fracture of split composite at various locations. Typically, the splitting starts at a low load. As the load is increased, the splitting extends along the sample and more splitting occurs at other locations. Final fracture is catastrophic. These two types are often accompanied by delamination as well. The third is delamination. When no continuous ply exists as in some composite sheets, the delamination leads to the so-called "tensile shear" fracture (of lap joints). In Table 3, the three types of fracture will be referred to by "F", "S" and "D", respectively.

Table 3 summarizes the sample lay-up, fracture load, mode of fracture and the nominal and effective fracture stresses. The second values of fracture load in parentheses indicate the loads at which a large load drop was observed. This is considered to be the initiation load of a large delamination. The effective fracture stress was calculated by using the area of un-cut laminae. When all the laminae were pre-cut, the fracture load was divided by the area of a lap joint to obtain tensile shear stress. Splitting was the dominant mode when un-cut laminae are included, whereas delamination was observed for the samples with lap joints (with one exception).

When the splitting mode is observed, the final fracture always coincided with complete delamination, followed by fiber fracture within each split composite. Thus, the fracture load (stress) represents the start of macroscopic delamination. This is also the case for the delamination mode of fracture.

Observed range of effective fracture strength was 150 to 230 ksi when un-cut laminae are included. This agrees with typical values for carbon fiber-epoxy composites in the 0° direction. The tensile shear strength with one inch overlap was 1200 to 3500 psi, increasing with the thickness of composites. This range is also typical of epoxy adhesive joints.

In most tests, splitting occurred starting at less than a half of the fracture load. Assuming typical values of Poisson's ratio, 0.24, the applied stress, 100,000 psi, the transverse modulus, 10^6 psi and the longitudinal modulus of 28×10^6 psi, we find the transverse stress to be 860 psi (assuming no width relaxation due to grip holding action). This is several times smaller than typical transverse ultimate strength of similar composites, but this appears to be caused by the compression of the sample at the grips inducing transverse tensile stress.

Acoustic Emission

Figure 1 shows the plots of load vs. time and rms voltages of acoustic emission signals vs. time curves for Test No. 32. The sample in this test had lay-up E-3, a six-laminae composite with two three-laminae group pre-cut, overlapping 2". This sample failed completely in tensile shear; that is, delamination of the overlap area led to failure. Strong acoustic emission signals were detected coinciding with load drops and nearing the final fracture. Noticeable acoustic emission activities started at about one-third of the maximum load level. The peak amplitude distribution of acoustic emission signals for this portion of the test is shown in Figure 2a (55 to 90 s segment out of the recorded test duration of 170 s). The number of acoustic emission events was less than 80 and the lowest and highest observable events had the peak amplitude of 52 dB and 84 dB in reference to 1 μV, respectively. The average peak amplitude of detected acoustic emission events was about 60 dB. The amplitude distributions of the next two segments (90 to 125 s and 125 to 145 s segments) are given in Figure 2b and 2c. These showed basically similar distributions. However, the average peak amplitude was lowered to 58 dB and 53 dB, respectively, and a new peak at 40 to 50 dB range emerged. The high end of the peak amplitude distribution was also extended to

128 dB. However, the major part of acoustic emission events had the peak amplitude between 50 and 70 dB. The events above 80 dB were evenly distributed during the second segment, but more events were found at 88 ~ 108 dB during the third segment. The amplitude distributions of the last segment (145 to 170 s) that includes final fracture are shown in Figure 2d and 2e. The two distributions represent low and high amplitude ranges. The two peaks discussed above merged showing the highest activity at 50 dB. For this segment, although its activity was lower than lower amplitude peaks (at 45 and 55 dB), another peak was found at 95 dB, as shown in Figure 2e.

The duration of acoustic emission events was also analyzed and the results indicate that:

- Most (>95%) events with peak amplitude below 50 dB have event duration less than 150 μs.
- Average event duration of medium amplitude (50 ~ 75 dB) events is ~ 120 μs.
- High amplitude events of over 75 dB have event duration longer than ~ 200 μs.

Since this composite essentially has a single lap joint configuration, the stress concentration at the ends of overlapping laminae leads to Mode I and Mode II fracture. This causes delamination at A or B in Figure 3. The delamination grows toward the center of the overlapping area. As the applied load increases, delamination begins at the other end. They can also grow toward the loading ends of the sample (although such delamination was not observed in Sample No. 32.) From the above acoustic emission observation, the medium amplitude (50 ~ 75 dB) events appear to correspond to the initiation and slow growth of delamination. This is so deduced because initial acoustic emission events had the medium amplitude levels only and the fracture of carbon fibers is quite unlikely at the applied stress levels below 30 ksi. The high amplitude (>75 dB), long duration (>200 μs) events are attributed to originate from rapid advances of the delamination, accompanied by load drops. Since this sample failed by delamination, the only plausible mechanism for the observed events during the final fracture is massive delamination. Even at the final fracture, this sample was stressed to only 43 ksi, making the fiber fracture unlikely. Examination of the fractured sample also indicated no apparent fiber fracture. Moreover, the high amplitude events observed were invariably of long duration. If a fiber fracture were to generate such a high amplitude event, one would expect a very short duration signal due to the small diameter of carbon fibers (~ 7 μm). Even with a slow crack growth rate of 10 m/s, it takes only 0.7 μs to fracture 7 μm fiber. While resonance phenonena increased the duration of acoustic emission signals, it is difficult to expect over 200 μs events. Thus, we can rule out fiber fracture for these high amplitude events. The above interpretation is in agreement with References [8] and [9], but not with the authors who attribute high amplitude events to fiber fracture [10 and 11]. The low amplitude events were considered to be due to the friction of delaminated faces [8]. The present condition makes this interpretation attractive, although we have no direct evidence to support this hypothesis.

The load-time and rms voltage-time curves for Test No. 65 are shown in Figure 4. The sample had nine laminae, the middle three laminae being pre-cut. It exhibited delamination of the un-cut outer laminae, after which these delaminated laminae split and finally the split outer laminae failed during the catastropic failure. The center three laminae were not split even after the final fracture, indicating the splitting became significant only after the delamination.

Acoustic emission signals were detected starting at ~ 100 s or at 46 ksi. The peak amplitude distribution of the segment when acoustic emission was first observed (2 to 3 minutes, corresponding to stresses of 55.4 to 76.8 ksi) is shown in Figure 5a. Here, it peaks at 31 dB and decreases with increasing amplitude. The decrease below 31 dB is due to approaching threshold level (25 dB). It is significant that over 90% of acoustic emission events have amplitude below 50 dB. About a half of the detected events exhibited less than 50 μs event duration. These short, low amplitude events cannot be attributed to delamination, which emits mostly in the amplitude range of 50 to 70 dB. Friction of delaminated faces cannot occur before substantial delamination takes place. In this sample, splitting started after the load drop due to a large delamination (at 350 s). The only likely source of low amplitude acoustic emission is then the fracture of carbon fibers. Lorenzo and Hahn [9] showed that the average peak amplitude level due to the fracture of a carbon fiber bundle is 35 dB. The present finding is in accord with their observation.

When this sample was loaded to 156 ksi, a load drop and delamination were observed. The peak amplitude distribution of this segment when acoustic emission became strong (6.67 to 7 minutes, corresponding to stresses of 140 to 156 ksi) is shown in Figure 5b, Here, a bimodal distribution with peaks at 33 dB and 52 dB was observed. More than a half of the events had the event duration longer than 150 μs. It is apparent that about 50% of acoustic emission events are similar to those observed at lower stresses, while the remainder can be attributed to delamination, which emits mostly in the amplitude range of 50 to 70 dB. Thus, we conclude that the amplitude distribution (Figure 5b) arises from the fracture of carbon fibers and the delamination.

The third type of acoustic emission behavior is illustrated in Figure 6 (Test No. 66). This sample was a seven-lamina composite, the center single lamina of which is pre-cut. In the failed sample, no delamination was detected. One major and two minor splitting were noted. The final fracture was due to fiber breakages at both ends (at the end of grip tabs). Acoustic emission started at the stress of 47.5 ksi. The peak amplitude distribution of acoustic emission signals from the start to 430 s (fractured at 440 s) is given in Figure 7a. A prominent peak at 33 dB is again evident. The average peak amplitude level is about 35 dB and a higher amplitude tail extended to 78 dB (maximum in the present setting). However, acoustic emission events with amplitude levels above 45 dB constituted less than 10%. The average event duration was about 35 μs. These short, low amplitude signals are again expected to arise from the fracture of carbon fibers as in the case of Test No. 65. The peak amplitude distribution from the initial segment (90 to 240 s) is given in Figure 7b. Except for the height of the distribution curve, it is nearly identical to Figure 7a, implying that mechanisms of acoustic emission are also similar. The peak amplitude distribution from 430 s to the end of the test is given in Figure 7c. Again, the results are remarkably similar to the two curves shown together. However, the number of events above 70 dB is higher, reflecting the fact that the final fracture is included in this segment.

In Figure 7a to 7c, it should be pointed out that events having the amplitude levels of 45 to 65 dB are always present. These were observed from the early stages to the final fracture. These medium amplitude signals are apparently due to splitting since no delamination was detected even in the fractured sample. These signals contribute to large spikes in the rms voltage-time curve (Figure 6) and their numbers are comparable to that of delamination-induced acoustic emission signals (Figure 2a). When a cross plot of peak amplitude and event duration was obtained using a POSTPRO program from AET, a general trend of longer event duration with higher peak amplitude was observed. When the peak amplitude is slightly above 50 dB, the event duration of all higher amplitude events exceeds 200 μs. Comparable long event duration for delamination induced signals was observed only for amplitude levels higher than 60 to 75 dB. In addition, a considerable number of events below 40 dB with the event duration of over 100 μs were also detected. These appear to be due to the splitting since the low amplitude events from fiber fracture have been shown to last no more than 100 μs in the discussion above. These findings are not

surprizing, as splitting is macroscopic crack propagation in the resin matrix at very low stresses. The splitting also propagates slowly and longer acoustic emission event duration is therefore expected. This topic needs to be studied further using other sample configurations that promote stable crack propagation along the fibers in unidirectional composites. This parameter may assist in discriminating between splitting and delamination, which produce similar amplitude acoustic emission events.

CONCLUSIONS

The present experiment shows that acoustic emission signals provide indications of different fracture processes in composites. The following conclusions have been reached using peak amplitude distribution and event duration of acoustic emission signals together with specially designed carbon fiber epoxy composite samples.

- The short duration (< 100 μs), lower amplitude signals (< 50 dB) signify carbon fiber fracture, which is found in unidirectional composites containing un-cut laminae at stresses exceeding ~ 50 ksi.
- The medium amplitude signals ($50 \sim 70$ dB) with an average event duration of ~ 120 μs indicate the initiation and slow growth of delamination. These were detected in composites with a lap-joint and in those with pre-cut mid-laminae.
- High amplitude vents (> 70 dB) have long (> 200 μs) event durations and are caused by rapid advances of delamination. These were typically observed during massive delamination accompanied by a load drop.
- Splitting or cracking along the fibers produces low to medium amplitude events with a long event duration (> 100 μs). This type of acoustic emission signals has overlapping characteristics with those of delamination and needs further delineation of distinguishing parameters.
- Delaminated samples also emit acoustic emission signals with amplitudes in the range of $40 \sim 50$ dB and event duration < 150 μs. These appear to arise from the friction of delaminated faces.

ACKNOWLEDGEMENTS

This research was supported by Hughes Aircraft Co. and by the Office of Naval Research, to which the author is most grateful. Assistance of Mr. Steve Jensen is greatly appreciated.

REFERENCES

1. Drouillard, T. F. and Hamstad, M. A., "A Comprehensive Guide to Literature on Acoustic Emission from Composites," *Proc. First International Symposium on Acoustic Emission from Reinforced Plastics*, CARP/Soc. Plastics Industry, New York, Sec. 6, pp. 1-60 (1983).
2. Belchamber, R. M., et al., "Evaluation of Pattern Recognition Analysis of Acoustic Emission from Stressed Polymers Composites," *J. Acoustic Emission*, 4(4), pp. 71-83 (1985).
3. Chan, R. W. Y., et al., "Classification of Acoustic Emission Signals Generated during Welding," *Acoustic Emission*, 4(4), pp. 115-123 (1985).
4. Ohtsu, M. and Ono, K., "Pattern Recognition Analysis of Magneto-mechanical Acoustic Emission Signals," *J. Acoustic Emission*, 3(2), pp. 69-80 (1984).
5. Reifsnider, K. L., ed., *Damage in Composite Materials*, ASTM STP 775, Amer. Soc. Testing and Materials, Philadelphia (1982).
6. *Effects of Defects in Composite Materials*, ASTM STP 836, Amer. Soc. Testing and Materials, Philadelphia (1984).
7. Johnson, W. S., ed., *Delamination and Debonding of Materials*, ASTM STP 876, Amer. Soc. Testing and Materials, Philadelphia (1985).
8. Gustafson, C.-G and Seldén, R. B., "Monitoring Fatigue Damage in CFRP using Acoustic Emission and Radiographic Techniques," *Delamination and Debonding of Materials*, ASTM STP 876, W. S. Johnson, ed., Amer. Soc. Testing and Materials, Philadelphia, pp. 448-464 (1985).
9. Lorenzo, L. and Hahn, H. T., "Acoustic Emission Study of Fracture of Fiber Embedded in Epoxy Matrix," *Proc. First International Symposium on Acoustic Emission from Reinforced Plastics*, CARP/Soc. Plastics Industry, New York, Sec. 2, pp. 1-13 (1983).
10. Wadia, J. R., "Acoustic Emission Applications," Dunegan/Endevco, San Juan Capistrano, CA (1978).
11. Awerbuch, J., et al., "Monitoring Damage Accumulation in Filament-wound Graphite/epoxy Laminate Coupons during Fatigue Loading through Acoustic Emission," *Proc. First International Symposium on Acoustic Emission from Reinforced Plastics*, CARP/Soc. Plastics Industry, New York, Sec. 2, pp. 1-30 (1983).

TABLE 1. Composite properties specifications.

Fiber	Tensile strength	350,000 psi
	Tensile modulus	52,000 psi
	Ultimate elongation	0.7%
	Density	1.82
Resin	Density	1.219
	Glass transition	306° F
	Tensile strength	10,600 psi
	Tensile modulus	600,000 psi
	Ultimate elongation	2.9%
	Poisson's ratio	0.35
Lamina	Fiber volume content	60%
	Width	6"
	Thickness	0.005"

TABLE 2. Lay-up geometry.

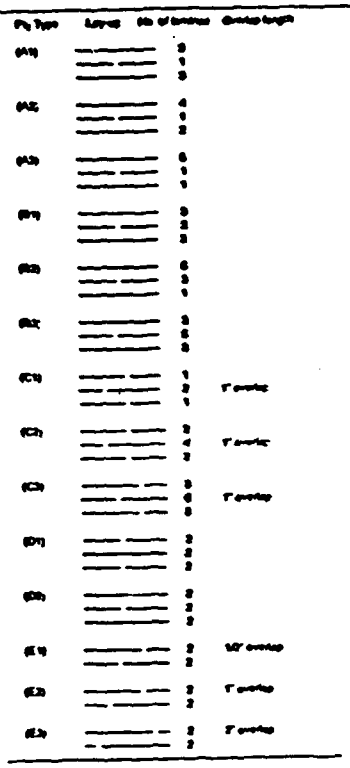

TABLE 3. Mechanical test data.

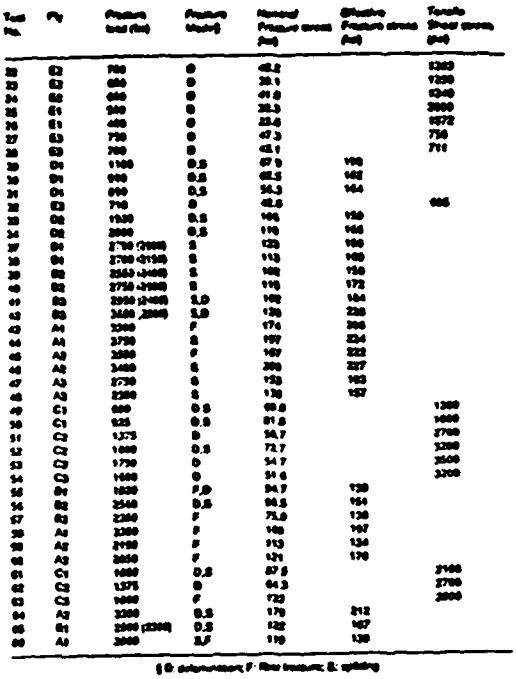

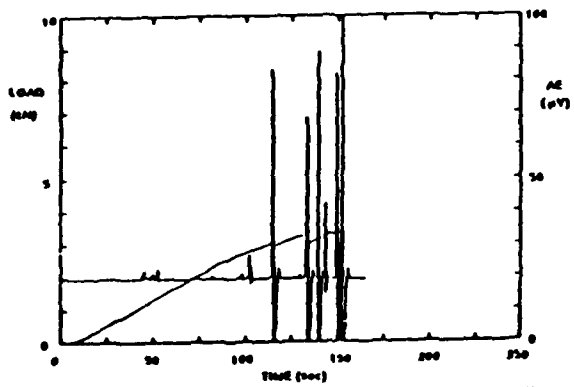

FIGURE 1. Load vs. time and the rms voltages of acoustic emission signals vs. time plots for Sample No. 32.

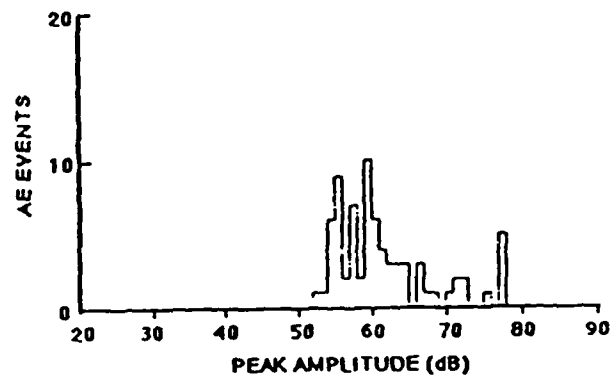

FIGURE 2a. The peak amplitude distribution of acoustic emission signals for the segment of 55 to 90 s for Sample No. 32 (cf. Figure 1). The reference level for the amplitude levels is 0 dB at 1 μV at the sensor output.

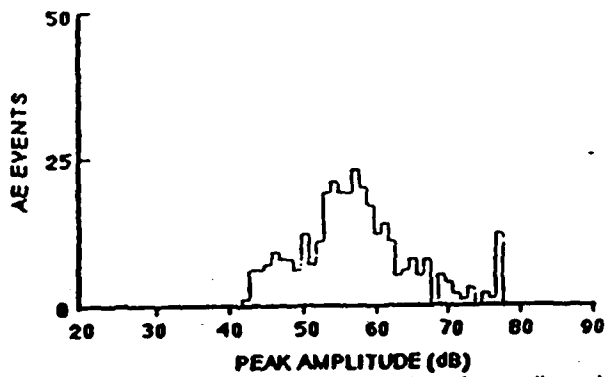

FIGURE 2b. The peak amplitude distribution of acoustic emission signals for the segment of 90 to 125 s for Sample No. 32 (cf. Figure 1). The reference level for the amplitude levels is 0 dB at 1 μV at the sensor output.

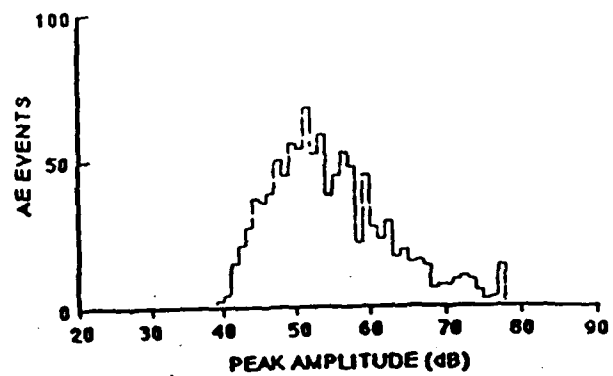

FIGURE 2c. The peak amplitude distribution of acoustic emission signals for the segment of 125 to 145 s for Sample No. 32 (cf. Figure 1). The reference level for the amplitude levels is 0 dB at 1 μ at the sensor output.

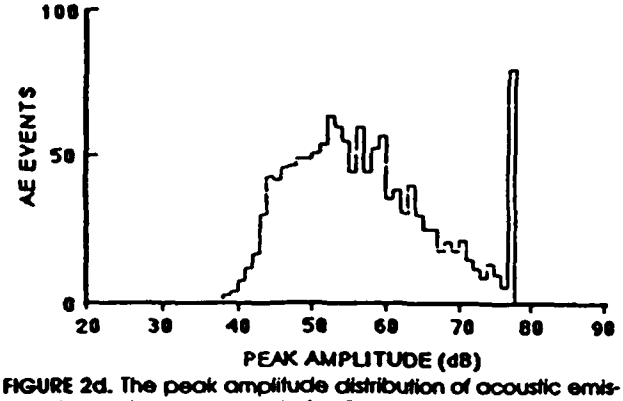

FIGURE 2d. The peak amplitude distribution of acoustic emission signals for the segment of 145 to 165 s for Sample No. 32 (cf. Figure 1). Low amplitude range. The reference level for the amplitude levels is 0 dB at 1 μV at the sensor output.

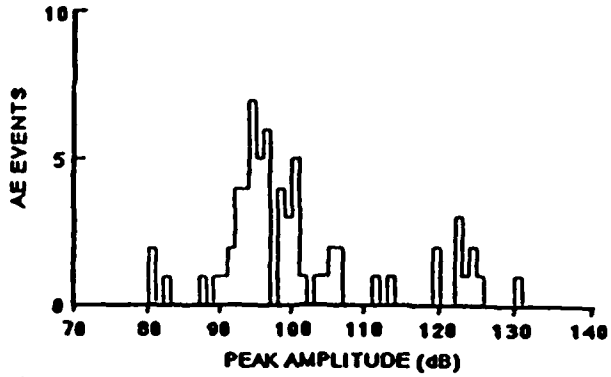

FIGURE 2e. The peak amplitude distribution of acoustic emission signals for the segment of 145 to 165 s for Sample No. 32 (cf. Figure 1). High amplitude range. The reference level for the amplitude levels is 0 dB at 1 μV at the sensor output.

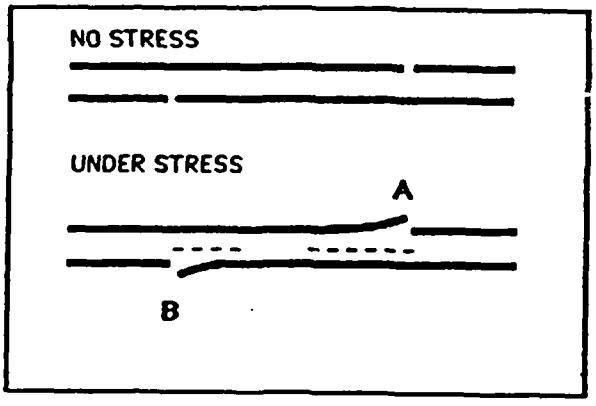

FIGURE 3. Delamination in type E lay-up composite. Both modes I and II fracture take place at A and B. Delamination normally advances toward the center of the sample.

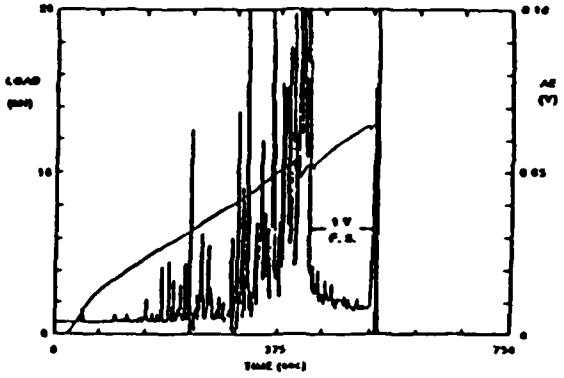

FIGURE 4. Load vs. time and the rms voltages of acoustic emission signals vs. time plots for Sample No. 65.

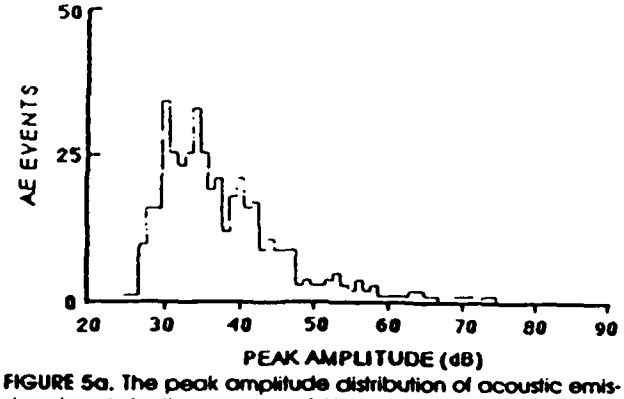

FIGURE 5a. The peak amplitude distribution of acoustic emission signals for the segment of 120 to 180 s for Sample No. 65 (cf. Figure 4). The reference level for the amplitude levels is 0 dB at 1 μV at the sensor output.

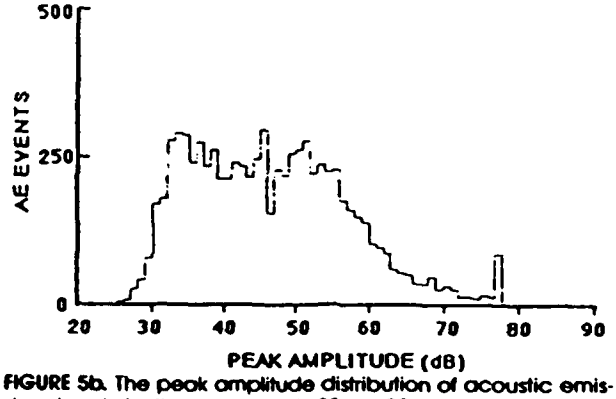

FIGURE 5b. The peak amplitude distribution of acoustic emission signals for the segment of 400 to 420 s for Sample No. 65 (cf. Figure 4). The reference level for the amplitude levels is 0 dB at 1 μV at the sensor output.

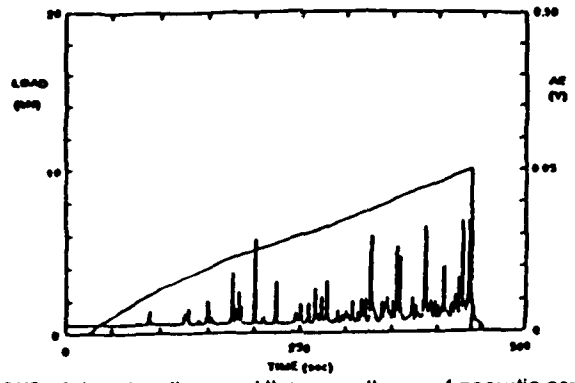

FIGURE 6. Load vs. time and the rms voltages of acoustic emission signals vs. time plots for Sample No. 66.

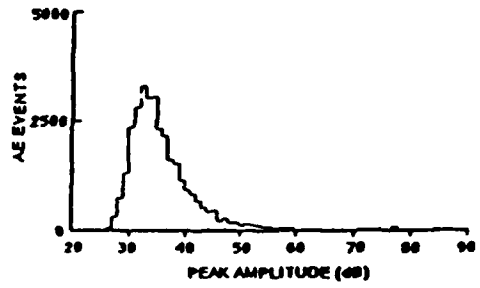

FIGURE 7a. The peak amplitude distribution of acoustic emission signals for the segment of 0 to 430 s for Sample No. 66 (cf. Figure 6). The reference level for the amplitude levels is 0 dB at 1 μV at the sensor output.

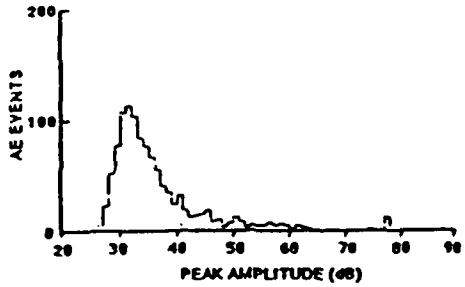

FIGURE 7b. The peak amplitude distribution of acoustic emission signals for the segment of 90 to 240 s for Sample No. 66 (cf. Figure 6). The reference level for the amplitude levels is 0 dB at 1 μV at the sensor output.

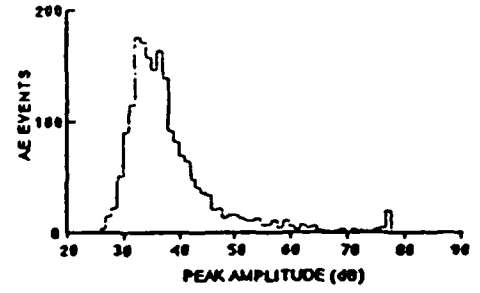

FIGURE 7c. The peak amplitude distribution of acoustic emission signals for the segment of 430 to 453 s for Sample No. 66 (cf. Figure 6). The reference level for the amplitude levels is 0 dB at 1 μV at the sensor output.

END

10-86

DTIC